# Versatile Patterns in the Actin Cortex of Motile Cells: Self-Organized Pulses Can Coexist with Macropinocytic Ring-Shaped Waves

Arik Yochelis,[1,2,*] Sven Flemming,[3] and Carsten Beta[3]
[1]Department of Solar Energy and Environmental Physics, Blaustein Institutes for Desert Research, Ben-Gurion University of the Negev, Sede Boqer Campus, Midreshet Ben-Gurion 8499000, Israel
[2]Department of Physics, Ben-Gurion University of the Negev, Be'er Sheva 8410501, Israel
[3]Institute of Physics and Astronomy, University of Potsdam, Potsdam 14476, Germany

(Received 24 March 2022; accepted 3 August 2022; published 19 August 2022)

Self-organized patterns in the actin cytoskeleton are essential for eukaryotic cellular life. They are the building blocks of many functional structures that often operate simultaneously to facilitate, for example, nutrient uptake and movement of cells. However, identifying how qualitatively distinct actin patterns can coexist remains a challenge. Using bifurcation theory of a mass conserved activator-inhibitor system, we uncover a generic mechanism of how different actin waves—traveling waves and excitable pulses—organize and simultaneously emerge. Live-cell imaging experiments indeed reveal that narrow, planar, and fast-moving excitable pulses may coexist with ring-shaped macropinocytic actin waves in the cortex of motile amoeboid cells.

DOI: 10.1103/PhysRevLett.129.088101

In biological cells, many functional processes take place simultaneously. Key examples are observed in the actin cytoskeleton of eukaryotic cells, which is a dense, dynamic biopolymer network located at the inner face of the plasma membrane. It provides the basis for important cellular functions, such as nutrient uptake, motility, and division. They rely on self-organized space-time patterns of cortical activity [1–7], both at the level of the actin cytoskeleton and in the upstream biochemical and mechanical signaling pathways [8–22]. These patterns often appear simultaneously and are abundantly observed in many cell types, such as neurons, dendritic cells, and neutrophils [23–25]. Thus, understanding how cells can generate and robustly maintain qualitatively different coexisting cortical patterns is fundamental not only to cellular life and its pathologies, such as cancer [23,26], but can also serve as a roadmap to the emerging field of synthetic biology, for which minimal candidate systems are required to robustly mimic intracellular spatiotemporal behaviors [27].

While previous research has primarily addressed the emergence of cortical actin waves that exhibit well-defined wavelengths or temporal periods [6,19,24,25,28–31], the coexistence of different patterns has been largely ignored and remains poorly understood. In this Letter, we first use an actin conserving, lumped activator-inhibitor model together with bifurcation theory to uncover a generic mechanism of wave organization, by which excitable pulses and oscillatory traveling waves emerge and coexist. The mechanism is discussed in dynamical system terms of limit cycles, homoclinic and heteroclinic orbits that correspond to propagating nonlinear wave solutions in a comoving coordinate frame. We then present experimental evidence from microscopy recordings of giant amoeboid cells, showing that different types of dynamical wave patterns can be indeed simultaneously maintained in the actin cortex of living cells.

*Emergence of actin waves and pulses.*—Intracellular actin dynamics involves multiple spatiotemporal feedbacks ranging from the molecular level of protein kinetics to mechanical membrane deformation [24,25,32–35]. Yet, it has already been shown that fundamental insights into actin wave dynamics can be obtained by approximate descriptions in terms of reaction-diffusion systems that reduce the complexity of the actin cortex to a small number of key components and incorporate their most salient interactions [36]. These include a conserved pool of actin that is either encountered in its monomeric form (G-actin) or may polymerize to filamentous cortical structures [filamentous actin (F-actin)]. In addition, F-actin may autocatalytically enhance its own formation, which reflects the well-known branching mechanisms and positive feedback to the activatory components of the upstream signaling pathway, such as PI3K and Ras [37]. On the other hand, the growth of filamentous structures is counterbalanced by inhibitory regulators, such as Coronin or Aip1 [38]. This is typically taken into account by an effective inhibitory component that is triggered in the presence of F-actin and downregulates the rate of polymerization. An overall schematic representation of the components and their interactions is displayed in Supplemental Material [40], Fig. S1. In general, due to autocatalytic growth and nonlinear feedback, multiple stable states may emerge that are characterized by different F-actin concentrations. From the study of circular dorsal ruffles, it is known that at least two stable

 

uniform states can coexist (bistability) [36]. In what follows, we first show that the analysis of such kinetics predicts coexistence between traveling waves and excitable planar pulses, where the latter can appear only in large cells which we, secondly, indeed confirmed in experiments.

To explicitly address the coexistence of traveling waves (TWs) and excitable pulses (EPs), we consider, without loss of generality, a reduced actin model [39] (for details see the Supplemental Material [40], Sec. S1) that can be seen as a specific realization of the reaction scheme presented in Supplemental Material [40], Fig. S1. We denote the F-actin concentration as $N(x,t)$, G-actin as $S(x,t)$, and the inhibitor as $I(x,t)$, so that the model phase space is spanned by $\mathbf{P}=(N,S,I)$. Three uniform solutions $\mathbf{P}_*^0=(N_*^0,S_*^0,I_*^0)$ and $\mathbf{P}_*^\pm=(N_*^\pm,S_*^\pm,I_*^\pm)$ exist (see the Supplemental Material [40], Eq. S3). In general, actin conservation implies that $L^{-1}\int_L\{N+S\}dx=A$, where $A$ is the total actin concentration, and $L$ is the domain length. In what follows, both will be used as control parameters. As G-actin monomers are inherently present, the G-actin-dominated state $\mathbf{P}_*^0$ always exists and is linearly stable, while the two states $\mathbf{P}_*^\pm$ coexist for $A>A_{\mathrm{SN}}$ [39], where $\mathbf{P}_*^-$ is linearly unstable, and $\mathbf{P}_*^+$ is linearly stable for $A>A_W$; see the bifurcation diagram in Figs. 1(a) and 1(b). The condition $A>A_W$ thus designates a bistable regime, where front solutions connecting $\mathbf{P}_*^0$ and $\mathbf{P}_*^+$ may form [36]. Here, we concentrate on the instabilities of the $\mathbf{P}_*^+$ state that occur as $A$ is decreased. The analysis is performed using the spatial dynamics methodology that combines bifurcation theory and numerical continuation using Ref. [41], and the results are summarized in Fig. 1; see also the Supplemental Material [40] for technical details, Sec. S2.

As $A$ is decreased, the uniform stable steady state $\mathbf{P}_*^+$ undergoes a wave (also known as finite wave number Hopf) instability at $A_W$, giving rise to traveling waves with wave number $k=k_W$; see the dispersion relation in the left panel of Fig. 1(a). In the bifurcation diagram in Fig. 1(b), the primary $\mathrm{TW}_{\lambda_c}$ branch that emerges from $A_W$ is displayed as a function of $A$ (green line). Each point along the $\mathrm{TW}_{\lambda_c}$ branch is associated with a periodic solution (with wavelength $\lambda_c=2\pi/k_W$) and plotted as the maximal value of the $N$ component. These TW solutions bifurcate (supercritically) toward the unstable direction of $\mathbf{P}_*^+$ and are initially stable. According to the standard theory [42], after the bifurcation is exceeded, i.e., as $A$ is decreased below $A_W$, additional TWs with a larger wavelength than $\lambda_c$ ($\lambda>\lambda_c$) emerge from the uniform state $\mathbf{P}_*^+$ (see the Supplemental Material [40], Fig. S3), in accordance with the dispersion relation [see Fig. 1(a)]. Importantly, the emergence of additional TWs is not related to the instability as the primary $\mathrm{TW}_{\lambda_c}$ branch, and thus, all secondary TWs are initially unstable although they may gain stability far from their emergence points. Additionally, standing waves (SWs) also bifurcate from $A_W$ (see the Supplemental Material [40], Sec. S2), as the standard theory of finite

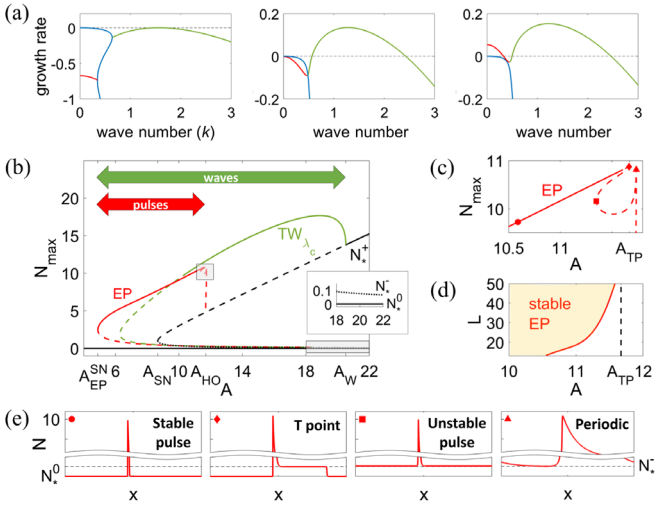


FIG. 1. Analysis of model system Supplemental Material [40], Eq. S1, for waves and pulses. (a) Perturbation growth rates at selected values of the total actin concentration, $A$. From left to right: the wave onset (green) at $A=A_W\simeq 20.5$, the wave unstable regime with HO neutral (red) at $A_{\mathrm{HO}}\simeq 11.7$, and an additional unstable regime at $A=11$, where waves and HO are both unstable. The blue curve indicates real valued dispersion relations while the green and red curves are complex conjugated (i.e., having identical real parts), meaning that the total number of three growth rate curves is always preserved. (b) Bifurcation diagram showing the branches of primary traveling wave solutions ($\mathrm{TW}_{\lambda_c}$) and EPs in periodic domains $L=\lambda_c=2\pi/k_W\simeq 4$ and $L=1000$, respectively. The branches are shown in terms of the maximal value of F-actin, $N$; solid lines indicate the linear stability regions of the solutions along the branch with respect to multiple copies of the wavelength. The inset shows an enlargement of the uniform solutions as indicated by the bottom shaded region. (c) Enlargement of the EP solutions about their origin near the $T$-point, $A=A_{\mathrm{TP}}$, (see top shaded region). (d) Stability of EPs with respect to the domain size $L$. (e) EP profiles along the branch in (c).

wave number Hopf instability predicts [43]. However, since SWs do not play any fundamental role in the context of EPs, we only show their coexistence in Supplemental Material [40] Figs. S2 and S3 while explicit analysis will be discussed elsewhere. Upon an increase of the domain size to cover multiple copies of TWs, a secondary instability of the Eckhaus-Benjamin-Feir type [44,45] destabilizes the TW solutions. For example, the instability onset for $\mathrm{TW}_{\lambda_c}$ saturates at $A\simeq 10.75$ for $L\sim O(10\lambda_c)$ [the instability onset is marked in Fig. 1(b) by the transition from a solid to a dashed line; see also Supplemental Material [40], Fig. S3].

An increase in the domain size is also related to the emergence of homogeneous oscillations (HO) at $A=A_{\mathrm{HO}}$ (in addition to TWs) for which the wave number vanishes and the wavelength diverges; see the dispersion relation in the middle panel of Fig. 1(a). Numerically, it is impossible to implement infinite domains, but the typical approximation

by periodic boundary conditions holds for such purposes. The continuation of periodic solutions from $A_{\mathrm{HO}}$, in a large domain $L = 1000 \gg \lambda_c$ [red line in Fig. 1(b)], shows that far from the onset, these solutions eventually develop into EPs. This evolution is depicted in Fig. 1(c), with the respective profiles along the branch in (c) displayed in panel (e). Up to the first sharp fold (homoclinic bifurcation in space) on the right (indicated by a triangle), the solutions are indeed periodic (with the period being as large as the domain size), and thus, at large amplitudes, they correspond to a broad pulselike state; see Fig. 1(c) and the rightmost profile in (e). The branch then proceeds to the left and up to another fold (indicated by a rectangle), where the profile approaches a genuine pulse solution [see panel (e)], yet this solution is unstable since it is embedded in the background of the unstable $\mathbf{P}_*^-$ state as $x \to \pm\infty$. Finally, after another fold at $A_{\mathrm{TP}}$ (indicated by a diamond), the branch extends to the left (toward $A_{\mathrm{EP}}^{\mathrm{SN}}$), and within this range, stable EPs emerge (as shown, for example, at the location indicated by a dot). Notably, the latter are embedded in the background of $\mathbf{P}_*^0$, as shown by the respective leftmost profile in (e). The speeds of EPs are larger than the speeds of all TWs, as demonstrated in Supplemental Material [40], Fig. S4. We note that near bifurcation onsets [43,46,47], this behavior is generic and not related to the specific choice of our model; see also the Supplemental Material [40], Sec. S3. Far from the TW bifurcation onset, linear stability regimes do depend on model details. Nevertheless, TWs with certain wavelengths will always coexist with EPs in some range of parameters.

The transition from unstable to stable EP solutions corresponds to a generic global bifurcation that is also of codimension 2 and on an infinite line, also known as the $T$-point [48,49]. This bifurcation designates the merging of two EPs (homoclinic orbits in space), creating a double front state (heteroclinic cycle in space) connecting bidirectionally (biasymptotically) two uniform solutions $\mathbf{P}_*^{\pm}$ as $x \to \pm\infty$ [50–52]. It is then straightforward to see that while on large domains, the stability onset of EP is close to $A_{\mathrm{TP}}$, on small domains, where the excitation width of EP is on the order of the domain size, the onset shifts to lower $A$ values, as shown in Fig. 1(d). This shift is associated with a structural change as the solutions depart from their solitary nature in space, becoming limit cycles (in space) rather than homoclinic orbits [48], see also Fig. 1(e). We refer the reader to the Supplemental Material [40], Sec. S2, specifically to Fig. S5, for further details on the pulse instability in domains of intermediate size, $O(\lambda_c) < L < O(10\lambda_c)$, and the relation to pulse splitting [39] and the backfiring phenomena [49,53–56]. Next, we show that planar EPs can indeed coexist with other wave patterns in the cortex of amoeboid cells if their size is increased.

*Experimental observation of planar pulses.*—A well-established model organism to study the dynamics of the actin cortex is the social amoeba *Dictyostelium discoideum*. In *D. discoideum*, actin waves were reported more than 20 years ago [57], and they have been intensively studied with respect to their dynamics, structure, and biochemical composition [8,10,58,59]. At the cytoskeletal level, these waves consist of traveling domains of increased F-actin concentration that are surrounded by a dense ring of F-actin. They resemble planar macropinocytic patches, i.e., functional structures that facilitate cellular liquid uptake but cannot evolve into full three-dimensional cups due to the rigid cover slip surface [60,61]. A particular advantage of the *D. discoideum* model system is the possibility to increase its cell size by electric-pulse-induced cell fusion, so that actin wave dynamics can be observed over large intact cell cortices independent of boundary effects [62–65].

These well-known wave patterns have been mostly described for axenic cell lines that feed on a liquid growth medium by macropinocytic liquid uptake. To explore new regimes of cytoskeletal dynamics, we changed the growth conditions and cultured the commonly used axenic *D. discoideum* lab strain AX2 together with bacteria; see the Supplemental Material [40], Sec. S4, for details on the cell lines and culture conditions. When feeding on bacteria, cells strongly enhance their pseudopod-driven motility in order to increase their chances of finding localized food sources [66]. We thus expect pseudopod formation to compete with the formation of macropinocytic cups for the common actin pool. Also in this case, we observed macropinocytic actin waves that displayed the characteristic ring-shaped structure and meandering dynamics; see the Supplemental Material [40], Sec. S5, with Fig. S7 and the Supplemental Material, Movie 1. However, upon an increase in cell size, the cortical wave patterns exhibited an additional new feature that has not been observed in giant cells produced from axenically grown cells in the absence of bacteria. Namely, in addition to the well-known broad ring-shaped wave segments, we observed sharp planar traveling pulses that behaved like genuine excitable solitary waves and have hitherto not been observed. Details on our cell fusion and image acquisition protocols can be found in the Supplemental Material [40], Secs. S6 and S7, respectively.

Both types of wave patterns, the broad macropinocytic traveling waves and the sharp planar pulses, coexisted in the same giant cell, and in Fig. 2(a), we show that they are distinct from each other in their profiles and propagation speeds; see also the Supplemental Material, Movie 2 [40]. The planar pulses propagated at a higher speed than the broad traveling waves, and their profile was sharply peaked as compared with the wider profile of the traveling waves, which exhibited characteristic actin peaks at their leading and trailing edges. The latter results from the ring-shaped structure of the frustrated cup [Fig. 2(b)], a feature that is well known from earlier reports [63]. The planar pulses typically emerged near the cell border and traveled straight

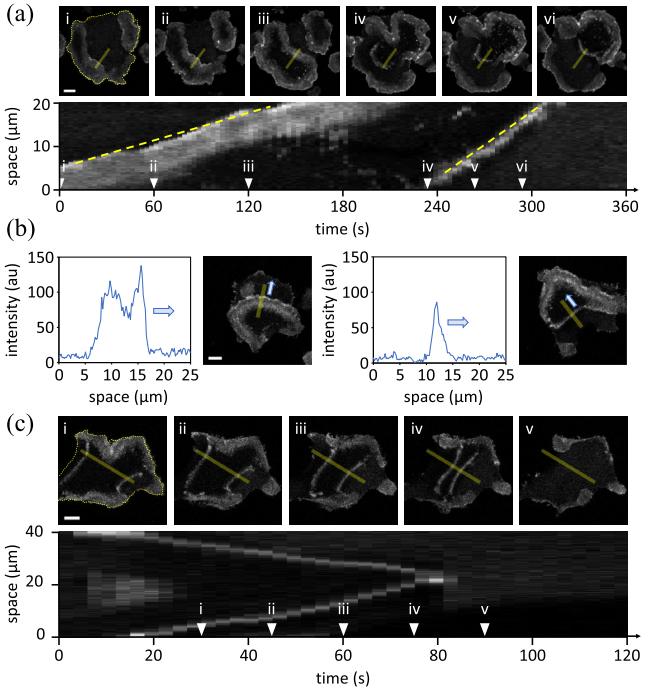


FIG. 2. (a) Coexistence of slowly moving broad actin waves and rapidly propagating planar pulses in the cortex of a giant *D. discoideum* cell. The kymograph on the bottom row was taken along the yellow line displayed in the snapshots above. The dashed yellow lines are visual guides, indicating the different speeds of the wave and the pulse propagation. (b) Actin profiles of a wave (left) and a pulse (right) together with their respective snapshots; the yellow lines show the position where the profile was recorded, and the arrow indicates the direction of the wave and the pulse propagation, respectively. (c) Head-on collision and mutual annihilation of two counterpropagating planar pulses. The kymograph on the bottom row was taken along the yellow line displayed in the snapshots above. Dashed yellow lines in panels (i) of (a) and (c) are visual guides that indicate the cell outline. All scale bars correspond to 10 $\mu$m.

across the substrate-attached bottom membrane. Upon head-on collision, the planar pulses mutually annihilated as expected; see Fig. 2(c) and the Supplemental Material, Movie 3 [40], for an example. We have also recorded the pulse dynamics in two different $z$ planes simultaneously to estimate the vertical extent of these structures, which reach at least 3 $\mu$m into the cytosol, and to ensure that they do not stem from imaging artifacts related to changes in the cell-substrate distance; for details see the Supplemental Material [40], Sec. S8.

*Discussion.*—Taken together, the rich and versatile spatiotemporal dynamics in the cell cortex is an essential part of actin-dependent cellular functions. Nevertheless, the coexistence of different cortical patterns is poorly understood as it is impossible to systematically decipher the underlying mechanisms based on visual and/or statistical inspections alone. In an attempt to address these fundamental mechanistic questions, we performed a bifurcation analysis of a mass conserved activator-inhibitor model of actin dynamics [36,39] [see Supplemental Material [40], Fig. S1], showing qualitatively that even in a lumped continuum-kinetic model that neglects most of the molecular details, essential features of pattern coexistence are revealed.

Several reductionist models of a similar kind have been proposed, hitherto, to describe the emergence of wave patterns in different organisms and cell types, such as human neutrophils [28], *C. elegance* embryos [67], or *Xenopus* oocytes [13]. In particular, cortical waves in *D. discoideum* have been intensely studied by reaction-diffusion type models of different complexity. While some of these models remain abstract and rely on one or two variables only [29,34,68], others focus on specific parts of the signaling pathway, such as small GTPases or phosphoinositide signaling [6,10,30,69], or they may even include several modules representing, for example, the dynamics of the actin cytoskeleton, the upstream signaling pathway, or polarity formation [70,71]. Even detailed molecular models have been proposed [72,73]. In contrast to these earlier works, our conclusions rely on a systematic analysis of how solutions are organized about a generic global bifurcation (the so-called $T$-point), which may arise also in other models with three or more variables that exhibit (i) monostability of a uniform state, (ii) coexistence of at least three uniform states, and (iii) mass conservation. Specifically, focusing on the total actin concentration as a control parameter and on nonlinear analysis in one space dimension (1D), we revealed how recurrent traveling waves may coexist with excitable pulses; see Fig. 1. Thus, our results provide a rigorous understanding of how coexisting wave patterns may emerge, and we believe that some of the above mentioned models will exhibit similar regimes of coexistence when analyzed with our approach. However, we emphasize that, while organization of solutions about the bifurcations is generic, the linear stability ranges depend on model details and may vary. Thus, a detailed study of sensitivity to transverse perturbations in 2D is also not in the scope of our present analysis, since these depend on kinetic and structural details, such as coupling to the membrane, cortex heterogeneity, noise, and constant changes in cell shape, which are typically not infinitesimal but constitute large perturbations.

Following the theoretical analysis, we showed experimental recordings of giant *D. discoideum* cells, demonstrating that distinct actin wave patterns can indeed coexist in the cortex of living cells. Specifically, we found that, in addition to the well-known wide, ring-shaped macropinocytic waves, a novel type of narrow and planar solitary pulse could be observed that revealed the typical excitable properties; see Fig. 2. In qualitative agreement with our theoretical predictions, these excitable pulses emerged upon an increase of the cell size and propagated faster than the ubiquitous traveling wave patterns. We believe

that, even though additional complex space-time patterns may coexist in cells, cf. Ref. [27], our results are a key prerequisite for analyzing and understanding fundamental questions of actin wave dynamics by mechanistically distinguishing coexisting wave forms. More broadly, our study of distinct coexisting wave types may also lead to a deeper understanding of cortical pathologies that could be related, for example, to cancerous phenotypes or uncontrolled tumor cell growth. It may furthermore inspire progress in the field of synthetic biology, where minimal, yet robust systems are required to reconstitute the essential features of self-organization in the cell cortex.

We thank Kirsten Sachse for technical assistance and Alexander Shevchenko for helpful discussions. We also thank the anonymous referees for their constructive comments. The research of Carsten Beta has been partially funded by the Deutsche Forschungsgemeinschaft (DFG), Project-ID No. 318763901—SFB1294.

*yochelis@bgu.ac.il

[1] G. J. Doherty and H. T. McMahon, Annu. Rev. Biochem. **78**, 857 (2009).
[2] N. W. Goehring and S. W. Grill, Trends Cell Biol. **23**, 72 (2013).
[3] J. P. Fededa and D. W. Gerlich, Nat. Cell Biol. **14**, 440 (2012).
[4] L. Blanchoin, R. Boujemaa-Paterski, C. Sykes, and J. Plastino, Physiol. Rev. **94**, 235 (2014).
[5] T. A. Masters, M. P. Sheetz, and N. C. Gauthier, Cytoskeleton **73**, 180 (2016).
[6] S. Fukushima, S. Matsuoka, and M. Ueda, J. Cell Sci. **132**, jcs224121 (2019).
[7] A. Michaud, Z. T. Swider, J. Landino, M. Leda, A. L. Miller, G. von Dassow, A. B. Goryachev, and W. M. Bement, Curr. Biol. **31**, R553 (2021).
[8] G. Gerisch, T. Bretschneider, A. Müller-Taubenberger, E. Simmeth, M. Ecke, S. Diez, and K. Anderson, Biophys. J. **87**, 3493 (2004).
[9] D. Shao, H. Levine, and W.-J. Rappel, Proc. Natl. Acad. Sci. U.S.A. **109**, 6851 (2012).
[10] T. Shibata, M. Nishikawa, S. Matsuoka, and M. Ueda, J. Cell Sci. **125**, 5138 (2012).
[11] W. Luo, C.-h. Yu, Z. Z. Lieu, J. Allard, A. Mogilner, M. P. Sheetz, and A. D. Bershadsky, J. Cell Biol. **202**, 1057 (2013).
[12] Y. H. Tee, T. Shemesh, V. Thiagarajan, R. F. Hariadi, K. L. Anderson, C. Page, N. Volkmann, D. Hanein, S. Sivaramakrishnan, M. M. Kozlov *et al.*, Nat. Cell Biol. **17**, 445 (2015).
[13] W. M. Bement, M. Leda, A. M. Moe, A. M. Kita, M. E. Larson, A. E. Golding, C. Pfeuti, K.-C. Su, A. L. Miller, A. B. Goryachev *et al.*, Nat. Cell Biol. **17**, 1471 (2015).
[14] G. Bloomfield, D. Traynor, S. P. Sander, D. M. Veltman, J. A. Pachebat, and R. R. Kay, eLife **4**, e04940 (2015).
[15] A. J. Lomakin, K.-C. Lee, S. J. Han, D. A. Bui, M. Davidson, A. Mogilner, and G. Danuser, Nat. Cell Biol. **17**, 1435 (2015).
[16] J. Negrete Jr, A. Pumir, H.-F. Hsu, C. Westendorf, M. Tarantola, C. Beta, and E. Bodenschatz, Phys. Rev. Lett. **117**, 148102 (2016).
[17] A. Diz-Muñoz, K. Thurley, S. Chintamen, S. J. Altschuler, L. F. Wu, D. A. Fletcher, and O. D. Weiner, PLoS Biol. **14**, e1002474 (2016).
[18] W.-J. Rappel and L. Edelstein-Keshet, Curr. Opin. Syst. Biol. **3**, 43 (2017).
[19] M. Hörning and T. Shibata, Biophys. J. **116**, 372 (2019).
[20] L. Stankevicins, N. Ecker, E. Terriac, P. Maiuri, R. Schoppmeyer, P. Vargas, A.-M. Lennon-Duménil, M. Piel, B. Qu, M. Hoth, K. Kruse, and F. Lautenschläger, Proc. Natl. Acad. Sci. U.S.A. **117**, 826 (2020).
[21] Y. Liu, E. G. Rens, and L. Edelstein-Keshet, J. Math. Biol. **82**, 28 (2021).
[22] N. Ecker and K. Kruse, PLoS One **16**, e0246311 (2021).
[23] J.-L. Hoon, W.-K. Wong, and C.-G. Koh, Mol. Cell. Biol. **32**, 4246 (2012).
[24] J. Allard and A. Mogilner, Curr. Opin. Cell Biol. **25**, 107 (2013).
[25] C. Beta and K. Kruse, Annu. Rev. Condens. Matter Phys. **8**, 239 (2017).
[26] J. D. Orth and M. A. McNiven, Cancer Res. **66**, 11094 (2006).
[27] A. Michaud, M. Leda, Z. T. Swider, S. Kim, J. He, J. Landino, J. R. Valley, J. Huisken, A. B. Goryachev, G. von Dassow *et al.*, J. Cell Biol. **221**, 8 (2022).
[28] O. D. Weiner, W. A. Marganski, L. F. Wu, S. J. Altschuler, and M. W. Kirschner, PLoS Biol. **5**, e221 (2007).
[29] S. Whitelam, T. Bretschneider, and N. J. Burroughs, Phys. Rev. Lett. **102**, 198103 (2009).
[30] Y. Arai, T. Shibata, S. Matsuoka, M. J. Sato, T. Yanagida, and M. Ueda, Proc. Natl. Acad. Sci. U.S.A. **107**, 12399 (2010).
[31] N. Nakamura and T. Shibata, Jpn. J. Ind. Appl. Math. **32**, 807 (2015).
[32] G. Gerisch, M. Ecke, D. Wischnewski, and B. Schroth-Diez, BMC Cell Biol. **12**, 1 (2011).
[33] E. Ben Isaac, U. Manor, B. Kachar, A. Yochelis, and N. S. Gov, Phys. Rev. E **88**, 022718 (2013).
[34] Y. Cao, E. Ghabache, and W.-J. Rappel, eLife **8**, e48478 (2019).
[35] N. Tamemoto and H. Noguchi, Soft Matter **17**, 6589 (2021).
[36] E. Bernitt, H.-G. Döbereiner, N. S. Gov, and A. Yochelis, Nat. Commun. **8**, 15863 (2017).
[37] A. T. Sasaki, C. Janetopoulos, S. Lee, P. G. Charest, K. Takeda, L. W. Sundheimer, R. Meili, P. N. Devreotes, and R. A. Firtel, J. Cell Biol. **178**, 185 (2007).
[38] H. C. Ishikawa-Ankerhold, G. Gerisch, and A. Müller-Taubenberger, Cytoskeleton **67**, 442 (2010).
[39] A. Yochelis, C. Beta, and N. S. Gov, Phys. Rev. E **101**, 022213 (2020).
[40] See Supplemental Material at http://link.aps.org/supplemental/10.1103/PhysRevLett.129.088101 for additional text, figures, and movies.
[41] E. J. Doedel, A. R. Champneys, T. Fairgrieve, Y. Kuznetsov, B. Oldeman, R. Paffenroth, B. Sandstede, X. Wang, and C. Zhang, Concordia University, http://indy.cs.concordia.ca/auto (2012).

[42] M. C. Cross and P. C. Hohenberg, Rev. Mod. Phys. **65**, 851 (1993).
[43] E. Knobloch, Phys. Rev. A **34**, 1538 (1986).
[44] B. Janiaud, A. Pumir, D. Bensimon, V. Croquette, H. Richter, and L. Kramer, Physica (Amsterdam) **55D**, 269 (1992).
[45] A. Yochelis, E. Knobloch, Y. Xie, Z. Qu, and A. Garfinkel, Europhys. Lett. **83**, 64005 (2008).
[46] M. Falcke, H. Engel, and M. Neufeld, Phys. Rev. E **52**, 763 (1995).
[47] D. Winterbottom, P. Matthews, and S. M. Cox, Nonlinearity **18**, 1031 (2005).
[48] P. Glendinning and C. Sparrow, J. Stat. Phys. **43**, 479 (1986).
[49] M. G. Zimmermann, S. O. Firle, M. A. Natiello, M. Hildebrand, M. Eiswirth, M. Bär, A. K. Bangia, and I. G. Kevrekidis, Physica (Amsterdam) **110D**, 92 (1997).
[50] J. Sneyd, A. LeBeau, and D. Yule, Physica (Amsterdam) **145D**, 158 (2000).
[51] M. Or-Guil, J. Krishnan, I. G. Kevrekidis, and M. Bär, Phys. Rev. E **64**, 046212 (2001).
[52] M. M. Romeo and C. K. Jones, Physica (Amsterdam) **177D**, 242 (2003).
[53] Y. Nishiura and D. Ueyama, Physica (Amsterdam) **150D**, 137 (2001).
[54] M. Argentina, O. Rudzick, and M. G. Velarde, Chaos **14**, 777 (2004).
[55] N. Manz and O. Steinbock, Chaos **16**, 037112 (2006).
[56] P. R. Bauer, A. Bonnefont, and K. Krischer, Sci. Rep. **5**, 16312 (2015).
[57] M. G. Vicker, W. Xiang, P. J. Plath, and W. Wosniok, Physica (Amsterdam) **101D**, 317 (1997).
[58] Y. Asano, A. Nagasaki, and T. Q. Uyeda, Cell Motil. Cytoskeleton **65**, 923 (2008).
[59] M. Jasnin, F. Beck, M. Ecke, Y. Fukuda, A. Martinez-Sanchez, W. Baumeister, and G. Gerisch, Structure **27**, 1211 (2019).
[60] G. Gerisch, M. Ecke, B. Schroth-Diez, S. Gerwig, U. Engel, L. Maddera, and M. Clarke, Cell Adhes. Migr. **3**, 373 (2009).
[61] D. M. Veltman, T. D. Williams, G. Bloomfield, B.-C. Chen, E. Betzig, R. H. Insall, and R. R. Kay, eLife **5**, e20085 (2016).
[62] G. Gerisch, M. Ecke, R. Neujahr, J. Prassler, A. Stengl, M. Hoffmann, U. S. Schwarz, and E. Neumann, J. Cell Sci. **126**, 2069 (2013).
[63] M. Gerhardt, M. Ecke, M. Walz, A. Stengl, C. Beta, and G. Gerisch, J. Cell Sci. **127**, 4507 (2014).
[64] Y. Miao, S. Bhattacharya, T. Banerjee, B. Abubaker Sharif, Y. Long, T. Inoue, P. A. Iglesias, and P. N. Devreotes, Mol. Syst. Biol. **15**, e8585 (2019).
[65] S. Flemming, F. Font, S. Alonso, and C. Beta, Proc. Natl. Acad. Sci. U.S.A. **117**, 6330 (2020).
[66] P. Paschke, D. A. Knecht, A. Silale, D. Traynor, T. D. Williams, P. A. Thomason, R. H. Insall, J. R. Chubb, R. R. Kay, and D. M. Veltman, PLoS One **13**, e0196809 (2018).
[67] J. B. Michaux, F. B. Robin, W. M. McFadden, and E. M. Munro, J. Cell Biol. **217**, 4230 (2018).
[68] S. Alonso, M. Stange, and C. Beta, PLoS One **13**, e0201977 (2018).
[69] M. A. Mata, M. Dutot, L. Edelstein-Keshet, and W. R. Holmes, J. Theor. Biol. **334**, 149 (2013).
[70] Y. Xiong, C.-H. Huang, P. A. Iglesias, and P. N. Devreotes, Proc. Natl. Acad. Sci. U.S.A. **107**, 17079 (2010).
[71] P. N. Devreotes, S. Bhattacharya, M. Edwards, P. A. Iglesias, T. Lampert, and Y. Miao, Annu. Rev. Cell Dev. Biol. **33**, 103 (2017).
[72] V. Khamviwath, J. Hu, and H. G. Othmer, PLoS One **8**, e64272 (2013).
[73] M. A. Avila Ponce de León, B. Félix, and H. G. Othmer, J. Theor. Biol. **527**, 110764 (2021).